ISSN 2277 – 8322

ANALYSIS OF THE STRUCTURAL BEHAVIOR OF FIBER REINFORCED CONCRETE BEAMS UNDER FLEXURAL LOADING

Krishna Kumar Thakur
M.Tech Scholar
Department of Civil Engineering
Mewar University, Chittorgarh
(Rajasthan)

Prof. Dr. Bhavesh Joshi
Associate Professor
Department of Civil Engineering
Mewar University, Chittorgarh
(Rajasthan)

Abstract- Due to the dense structure of ultra-high-performance concrete (UHPC), it is prone to explosive spelling at high temperatures. In this paper, flexural testing of UHPC and high-strength concrete (HSC) beams was carried out at room temperature and after being subjected to different levels of thermal exposure (300–500 °C). The cross-section of the beam specimen was 150 (width) × 200 (depth) mm, and its length was 1500 mm. The flexural and shear design of the beam specimens were carried out in accordance with the ACI 318M-14 code. All of the beams were singly reinforced with two #4 rebars (minimum reinforcement ratio) as a longitudinal tensile reinforcement at the bottom of the specimen and at an effective depth of 165 mm. The flexural load was applied using the three-point load method. The results show that, at room temperature and after being subjected to different thermal exposures, compared with the HSC specimens, the stiffness of the UHPC specimens in the post-cracking stage was relatively larger and the deflection under a given load was smaller. Moreover, whether at room temperature or after exposure to different thermal exposures, the ductility of the UHPC specimens was better than that of the HSC specimens.

Keywords: Ultra-high-performance concrete; flexural behavior; high temperature; ductility

I. INTRODUCTION

Concrete is the most widely used construction material because of its versatility, durability, and high compressive strength. However, conventional concrete possesses very low tensile strength and limited strain capacity, resulting in brittle failure and

crack propagation under tensile stresses. Reinforcement bars are generally used to resist tensile forces, but micro-cracks still develop within the concrete matrix.

Fiber Reinforced Concrete (FRC) is a composite material consisting of cement, aggregates, water, and randomly distributed discontinuous fibers. The addition of fibers enhances the post-cracking behavior and energy absorption capacity of concrete. Fibers act as crack arresters by bridging cracks and transferring tensile stresses across crack surfaces.

Different types of fibers such as steel fibers, glass fibers, polypropylene fibers, carbon fibers, and natural fibers are used depending on engineering requirements.

Concrete is strong in compression but weak in tension. Cracking occurs easily under tensile stress. To overcome this limitation, fibers are added to concrete.

Concrete is a cement-based composite material that uses cement combined with aggregates, additives, etc., to form a hydraulic cementations' material. Since the 1970s, due to the successful development of chemical admixtures (especially super-plasticizers) and the application of mineral admixtures (mainly ground granulated blast furnace slag, silica fume, fly ash, etc.), various special concrete products have been developed one after another. Familiar products include, for example, high performance concrete (HPC) and ultra-high-performance concrete (UHPC).

The American Institute of Concrete (ACI Committee 239) defines UHPC as "concrete that has a minimum specified compressive strength of 150 MPa and meets specific durability, tensile ductility, and toughness requirements. Many researchers point out that there are three key factors in the production of UHPC, including improved micro and macro properties of the matrix composition, maximum particle packing density, and minimum size defects. The typical composition of UHPC generally includes cement, fine aggregates, fiber, mineral additives, and super-plasticizer. The mix proportions of UHPC have several characteristics, including a low water-to-binder ratio, a large amount of very fine powders by using only fine sand for aggregates, a low water content (adding high-dose super-plasticizers), and the use of fibers. UHPC is

generally prepared by mixing its constituent materials with water, before setting and hardening it to form concrete with an ultra-high compressive strength, high tensile toughness, and excellent durability. At present, UHPC is applied in major engineering projects such as roads, bridges, and water conservancy projects.

II. EXPERIMENTAL STUDY

Materials:

The materials used in this study include water, cement, mineral admixtures (silica fume and ultra-fine silica powder), fine aggregates (quartz sand), chemical admixtures (super-plasticizer and viscous agent), fibers, and steel rebar's. The properties and sources of these materials are as follows:

- Water: general tap water that met the quality requirements of concrete mixing water.
- Cement: ordinary Portland Type I cement produced by the Taiwan Cement Corporation. Its specific gravity and fineness were 3.15 and 3400 cm^2/g, respectively.
- Silica fume: Elkem Microsilica 940U purchased from Taiwan Sika Co., Ltd., its specific gravity was 2.1, and its silicon dioxide (SiO_2) content was 92.4%.
- Ultra-fine silicon powder: purchased from Dawei Stone Industry Company (Jhubei, Taiwan), its specific gravity and silicon dioxide content were 2.73 and 92%, respectively, and the average particle size was 0.075–0.225 μm.
- Fine aggregate: purchased from Jinjing Silica Sand Co., Ltd.; it belonged to quartz sand and contained two different grades, namely Type A and Type B. The properties and composition of these fine aggregates are shown in **Table 1**, and the particle size distribution is shown in **Table 2**. Among the fine aggregates, 80% are type A and 20% are type B.
- Super-plasticizer: R-550, a product of Taiwan Sika Company that met the requirements of ASTM C494-81 Type F.
- Viscous agent: purchased from Guanghui Building Material Co., Ltd.
- Fiber: purchased from Gulili Co. Ltd., short micro steel fiber (according to ASTM A820) with a length of 13 mm and a diameter of 0.2 mm and polypropylene fiber

with a length of 12 mm and a diameter of 0.05 mm, as shown in **Figure 1**. The basic properties of the two fibers are shown in **Table 3**.

- Steel rebar: SD280W #3 and #4. Their various physical and mechanical properties are shown in **Table 4**.

Figure 1: The appearance of the fibers: **(a)** steel fibers and **(b)** polypropylene fibers.

Table 1: The properties and compositions of the fine aggregates.

	Physical Properties		**Chemical Composition**		
	Specific Gravity (S.S.D)	Water Absorption Rate (%) (S.S.D)	Silicion Dioxide (%)	Iron Oxide (%)	Aluminium Oxide (%)
Type A	2.65	0	99.82	0.01	0.03
Type B	2.65	0	99.84	0.02	0.03

Notes: S.S.D., Saturated-Surface-Dry.

Table 2: The particle size distribution of the fine aggregates.

Sieve No. (ASTM	**Partical Size (Mm)**	**Percentage Retained (%)**

E11-70)		**Type I**	**Type II**
20	850	0.04	-
30	600	20.15	-
40	425	67.83	-
50	300	11.81	-
60	250	-	0.05
70	212	0.17	13.39
100	150	-	36.55
140	106	-	32.39
200	75	-	12.73
270	53	-	3.61

Table 3: The physical and mechanical properties of the fibers.

Types of Fiber	**Length (mm)**	**Diameter (mm)**	**Density (g/cm2)**	**Elastic Modulus (Gpa)**	**Tensile Strength (Mpa)**	**Melting Point (*C)**
Steel Fibers	13	0.2	7.8	200	2000	-
Polypropylene Fibers	12	0.05	0.9	-	300	165

Table 4: The physical and mechanical properties of the steel rebar's.

Bar No.	**Nominal Dia. (mm)**	**Nominal Cross section**	**Rib Distance (mm)**	**Rib Height (mm)**	**Yield Strength (N/mm2)**	**Ultimate Strength (N/mm2)**

		Area (cm2)				
#3	9.53	0.713	8.3	0.7	334	464
#4	12.70	1.267	8.3	0.7	380	465

. Test Methods and Instrumentation:

The testing of the fresh and hardened properties of the UHPC was carried out according to the ASTM specifications listed in **Table 6**. The test age of the cylindrical specimen was 56 days, and an average of three specimens was taken. After the beam specimen had been cured, flexural tests at room temperature and after exposure to high temperatures were carried out in accordance with the ASTM C1609/C1609M-19a specification.

Table 6: The test methods of the fresh and hardened properties of the UHPC.

Property	**Experiment Method**
Unit Weight	ASTM C138
Slump	ASTM C143
Slump Flow	ASTM C1611
Compressive Strength	ASTM C39
Flexural strength	ASTM C1609/ C1609M-19a

At each target temperature, the control group and the experimental group have two beam specimens for flexural tests. The installation of the specimen is shown in **2**. An electro-hydraulic servo actuator with a maximum load of 6000 kN was used to apply a monotonic load, and an additional force sensor was installed to ensure the accuracy of the load data. The beam specimen was placed on the two supports of the testing machine and the load was applied using the three-point load method (with the use of the transfer steel beam to create the load position shown in **2**; the load was

added 15 cm from the center to the left and right). The load was gradually applied at a constant rate of 0.98 kN/s. Each loading time was ten seconds, and the load was maintained at a fixed value for five seconds. The deflection readings at each load step were recorded until the beam specimen failed so as to obtain the relationship curve between the central deflection and the applied load. At each stage of loading, the beam was carefully inspected with a magnifying glass to detect the first crack; then, the flexural load corresponding to the first crack was recorded.

Figure 2: The general flexural test setup for the beam specimens.

III. RESULTS AND DISCUSSION

The configuration of the stirrups of the beam specimen was limited to the shear span. Its purpose was to prevent the specimen from being damaged by shear failure and cause the specimen to fail in tension so as to compare the flexural behavior of different concrete beams. As the HSC and UHPC beam members were designed to have a relatively low reinforcement ratio, the two groups of beam specimens were a tensile failure, as shown in Figure 3. When the load reached the flexural cracking load of the beam, vertical cracks began to

appear in the pure bending moment area at the mid-span of the specimen, and the width was about 0.1–0.2 mm. As the load continued to increase, the steel fibers were pulled out one after another, the vertical cracks continued to extend upward, and their widths continued to increase to become obvious cracks. In addition, we could even hear the sound of fibers being pulled out, and we observed concrete fragments falling from the cracks. When the load exceeded the peak load, the load-bearing capacity of the specimen decreased significantly, while the crack width continued to increase and then penetrate the concrete on the compression side. The test results showed that when the surface of the concrete on the compression side in the pure moment zone flaked off, the residual load of the HSC beam could still be maintained for a period of time. The concrete strength of the UHPC was higher and steel fiber and polypropylene fibers were mixed. Therefore, the peak load and residual load of the UHPC specimen were significantly higher than those of the HSC. However, due to the configuration of the minimum reinforcement ratio, the failure of the UHPC beams was rapid, with a characteristic brittle cracking. The test results of the average peak load of the HSC and UHPC specimens at room temperature are shown in **Table** 7. It can be seen from **Table 7** that, at room temperature, the 56-day-old average peak load of the UHPC beam was significantly higher than that of the HSC beam, with a gap of 27.4 kN this result shows that the UHPC beam specimens made full use of the high tensile strength of the ultra-high-performance fiber-reinforced concrete, which benefited from the presence of steel fibers.

(a) (b)

Figure 3: The tensile failure in the flexural test of beam at room temperature: **(a)** the experimental group and **(b)** the control group.

Table 7: The flexural load of the beams at room temperature and after thermal exposure.

Designation	Average Peak Load (KN)	Average Residual Peak Load (KN)			Average Relative Residual Peak Load Ratio		
	Room Temperature	Target Temperature			Target Temperature		
		300*c	400*c	500*c	300 *c	400*c	500*c
C1	46.4	47.6	49.2	50.7	1.04	1.08	1.11
E1	73.8	75.3	69.3	76.8	1.02	0.94	1.04

The Results of Flexural Test of Beams after Different Thermal Exposures:

After the beam specimens were subjected to different thermal exposures and cooled, they were transported to the MTS universal testing machine in our large-scale structural laboratory for a three-point load test. After experiencing high temperatures, the beam specimens of the two groups of concrete still showed tensile failure. For example, **Figure 11** shows the tensile failure of a beam in a flexural test after being subjected to 400 °C.

Figure 4: The tensile failure in the flexural test of beams after being subjected to 400 °C: **(a)** the experimental group and **(b)** the control group.

The UHPC beams had a high compressive strength and were mixed with steel fiber and polypropylene fiber. There was only one vertical

flexural crack in their pure bending moment zone, and there was no obvious crushing and flake-off of the concrete surface on the compression side. In addition, when the beam of the experimental group reached the ultimate load, the flexural cracks quickly passed through the pressure zone, causing the specimen to break into two halves, as shown in Figure 5.

Figure 5: The fracture situation of the experimental group after being subjected to 400 °C.

The Ductility of the Beam Flexural Test after Different Thermal Exposures:

Ductility characterizes the ability of reinforced concrete components to absorb energy and undergo significant inelastic deformation and can be measured according to the curvature, rotation, or deflection of the component. Exposure to high temperatures has a significant impact on the mechanical properties of UHPC. In particular, high temperatures cause UHPC to exhibit brittleness. Therefore, it is necessary to further explore the influence of high temperatures on the ductility of UHPC beams. In order to simplify the calculation, the deflection ductility index is often used. The expressions shown below are commonly used as ductility indices:

$$\mu p=\Delta p\Delta,\ldots\ldots. (1)$$

$$\mu u=\Delta u\Delta y\ldots\ldots\ldots(2)$$

Among these, Δp is the mid-point deflection of the beam span under the peak load, Δy is the mid-point deflection of the beam span when the longitudinal reinforcement is yielded, and Δu is the mid-point deflection of the beam span under the ultimate load or the deflection corresponding to the load at 80–85% of the peak load from the descending branch of the load–deflection curve. Qi et al. proposed a new ductility index that divides the ultimate deflection by the flexural cracking deflection (Δcr) to characterize the ductility of a component after cracking:

$$\mu cr = \Delta u \Delta cr \ldots\ldots\ldots (3)$$

This study conducted a theoretical analysis on the ductility of the prepared beam specimens. When the longitudinal reinforcement of the beam yields, it reaches the yielding state. It can be considered that the prepared single-reinforced beam is basically in an elastic state. Therefore, the yield curvature of the critical section of the beam (ϕy) can be expressed as follows:

$$\phi y = fyE(1-k) \ldots..(4)$$

Where fy is the yield stress of steel rebar, Es is the modulus of elasticity of steel rebar, d is the effective depth of beam section, and k is the ratio of neutral axis depth to effective depth.

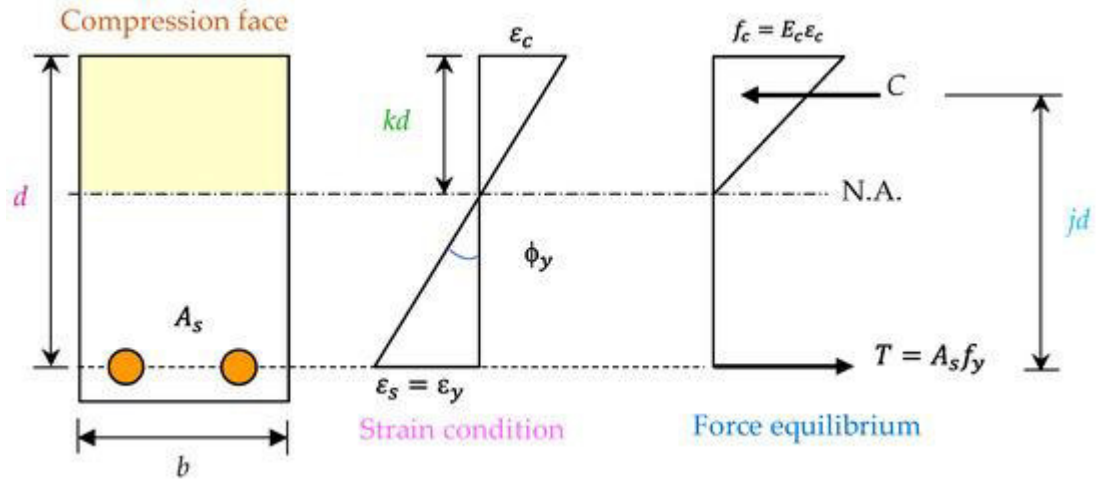

Figure 6: The stress and strain profiles of a typical reinforced concrete beam at the yielding state.

The stress and strain distribution of the beam in the ultimate state is

shown in Figure 6. The ultimate curvature (ϕu) of the critical section of the beam can be expressed as follows:

$$\phi u = \varepsilon uc = \beta 1 \varepsilon ua \ldots\ldots\ldots (5)$$

where εu is the ultimate strain of concrete, c is the depth of the neutral axis of the beam section in the ultimate state, $\beta 1$ is the ratio of depth of equivalent rectangular stress block to depth of the neutral axis, and a is the depth of equivalent rectangular stress block of the beam section.

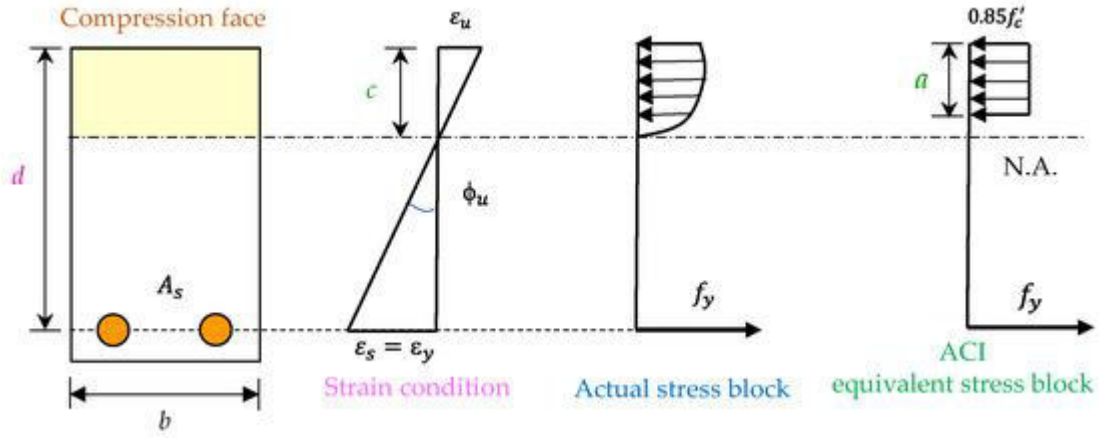

Figure 7: The stress and strain profiles of a typical reinforced concrete beam at the ultimate state.

Consider a simply supported beam that bears two concentrated loads at the center of the span. Its bending moment diagram and curvature diagram are shown in Figure 7.

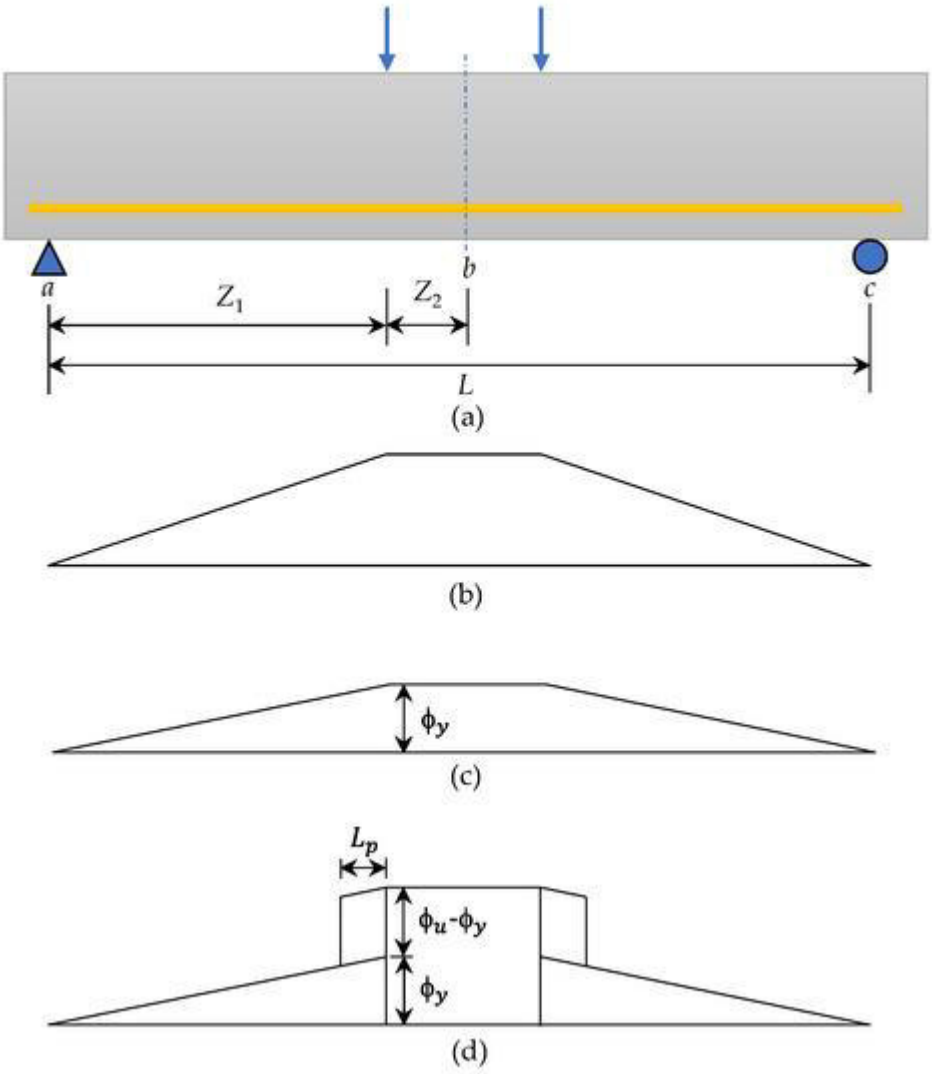

Figure 8: Schematic diagram of the curvature area theorem for obtaining a typical beam deflection: **(a)** load diagram, **(b)** bending moment diagram, **(c)** idealized curvature at the yielding stage, and **(d)** idealized curvature at the ultimate stage.

IV. CONCLUSIONS

According to the flexural behavior of the UHPC beams after being exposed to different levels of thermal exposure, the following conclusions can be drawn:

- After proper pre-drying treatment, the UHPC and HSC beam specimens did not spall even when exposed to a high temperature of 500 °C.
- SEM observation confirmed that the polypropylene fiber melted at high temperature, which increased the permeability of the UHPC matrix and released water vapor.

- At room temperature and after being subjected to different thermal exposures, compared with the HSC specimens, the stiffness of the UHPC specimens in the post-cracking stage was relatively larger and the deflection under a given load was smaller.
- The average relative residual peak load ratios of the UHPC beam specimens after being subjected to 300 and 400 °C were both as high as 0.94. In particular, as the target temperature reached 500 °C, the average residual load still increased, and the average residual peak load ratio was greater than one.
- The ductility of the UHPC specimens was better than that of the HSC specimens regardless of whether it was at room temperature or after exposure to high temperatures.
- Polypropylene and steel fibers can release pore pressure to a certain extent to prevent the UHPC matrix from spelling. Therefore, the UHPC beams incorporating hybrid polypropylene and steel fibers showed improved flexural performance after being subjected to different levels of thermal exposure. In addition, reducing the moisture content of the UHPC beams is an effective way to improve its spelling resistance.

The beam specimen in this study was configured as a single reinforced beam, which used the minimum reinforcement ratio to design the longitudinal tensile steel at the bottom of the specimen. Subsequent studies can be planned for different reinforcement ratios to further explore the flexural behavior of UHPC beams after high temperature. In addition, UHPC beams that are simultaneously subjected to load and high temperature can be planned to further explore the flexural behavior of UHPC beams.

REFERENCES

[1] Mindess, S.; Young, J.F.; Darwin, D. Concrete, 2nd ed.; Prentice-Hall: Upper Saddle River, NJ, USA, 2003.

[2] Metha, P.K.; Monteiro, P.J.M. Concrete; Microstructure, Properties and Materials, 3rd ed.; McGraw-Hill: New York, NY, USA, 2006.

[3] Shi, C.J.; Wu, Z.M.; Xiao, J.F.; Wang, D.H.; Huang, Z.Y.; Fang, Z. A review on ultra high performance concrete: Part I. Raw materials and mixture design. Constr. Build. Mater. 2015, 101, 741–751.

[4] Graybeal, B. Ultra-high-performance concrete connections for precast concrete bridge decks. PCI J. 2014, 49, 48–62.

[5] ACI 239R-18: Ultra-High Performance Concrete: An Emerging Technology Report (2018); American Concrete Institute: Farmington Hills, MI, USA, 2018.

[6] Larrard, D.F.; Sedran, T. Optimization of ultra-high-performance concrete by the use of a packing model. Cem. Concr. Res. 1994, 24, 997–1009.

[7] Wille, K.; Naaman, A.; Montesinos, G. Ultra-high performance concrete with compressive strength exceeding 150 MPa (22 ksi): A simpler way. ACI Mater. J. 2011, 108, 46–54.

[8] Díaz, J.; Gálvez, J.C.; Alberti, M.G.; Enfedaque, A. Achieving ultra-high performance concrete by using packing models in combination with nanoadditives. Nanomaterials 2021, 11, 1414.

[9] Abbas, S.; Nehdi, M.L.; Saleem, M.A. Ultra-high performance concrete: Mechanical performance, durability, sustainability and implementation challenges. Int. J. Concr. Struct. Mater. 2016, 10, 271–295.

[10] Sanjuán, M.Á.; Andrade, C. Reactive powder concrete: Durability and applications. Appl. Sci. 2021, 11, 5629.

[11] Yu, R.; Spiesz, P.; Brouwers, H.J.H. Mix design and properties assessment of ultra-high performance fiber reinforced concrete (UHPFRC). Cem. Concr. Res. 2014, 56, 29–39.

[12] Schmidt, M.; Fehling, E. Ultra-high-performance concrete: Research, development and application in Europe. ACI Spec. Publ. 2005, 228, 51–78.

[13] Du, R.Y.; Huang, Q.W.; Chen, B.C. Application and study of reactive powder concrete to bridge engineering. World Bridges 2013, 41, 69–74.

[14] Valikhani, A.; Jahromi, A.J.; Mantawy, I.M.; Azizinamini, A. Experimental evaluation of concrete-to-UHPC bond strength with correlation to surface roughness for repair application. Constr. Build. Mater. 2020, 238, 117753.

[15] Biswas, R.K.; Bin Ahmed, F.; Haque, M.E.; Provasha, A.A.; Hasan, Z.; Hayat, F.; Sen, D. Effects of steel fiber percentage and aspect ratios on

fresh and harden properties of ultra-high performance fiber reinforced concrete. Appl. Mech. 2021, 2, 28.

[16] He, J.; Chen, W.; Zhang, B.; Yu, J.; Liu, H. The mechanical properties and damage evolution of UHPC reinforced with glass fibers and high-performance polypropylene fibers. Materials 2021, 14, 2455.

[17] Kahanji, C.; Ali, F.; Nadjai, A. Structural performance of ultra-high-performance fiber-reinforced concrete beams. Struct. Concr. 2017, 18, 249–258.

[18] Yoo, D.-Y.; Banthia, N.; Yoon, Y.-S. Experimental and numerical study on flexural behavior of ultra-high performance fiber-reinforced concrete beams with low reinforcement ratios. Can. J. Civ. Eng. 2017, 44, 18–28.

[19] Hasgul, U.; Turker, K.; Birol, T.; Yavas, A. Flexural behavior of ultra-high-performance fiber reinforced concrete beams with low and high reinforcement ratios. Struct. Concr. 2018, 19, 1577–1590.

[20] Chalioris, C.E.; Kosmidou, P.-M.K.; Karayannis, C.G. Cyclic Response of Steel Fiber Reinforced Concrete Slender Beams: An Experimental Study. Materials 2019, 12, 1398.